Energy loss of pions and electrons of 1 to 6 GeV/c in drift chambers operated with Xe,CO_2(15%)

A. Andronic [a,1,2], H. Appelshäuser [b], C. Blume [a], P. Braun-Munzinger [a], D. Bucher [c], O. Busch [a], V. Cătănescu [d,b], M. Ciobanu [d,a], H. Daues [a], D. Emschermann [b], O. Fateev [e], Y. Foka [a], C. Garabatos [a], T. Gunji [f], N. Herrmann [b], M. Inuzuka [f], E. Kislov [e], V. Lindenstruth [g], W. Ludolphs [b], T. Mahmoud [b], V. Petracek [b], M. Petrovici [d], I. Rusanov [b], A. Sandoval [a], R. Santo [c], R. Schicker [b], R.S. Simon [a], L. Smykov [e], H.K. Soltveit [b], J. Stachel [b], H. Stelzer [a], G. Tsiledakis [a], B. Vulpescu [b], J.P. Wessels [c], B. Windelband [b], C. Xu [b], O. Zaudtke [c], Yu. Zanevsky [e], V. Yurevich [e]

[a] *Gesellschaft für Schwerionenforschung, Darmstadt, Germany*

[b] *Physikaliches Institut der Universität Heidelberg, Germany*

[c] *Institut für Kernphysik, Universität Münster, Germany*

[d] *NIPNE Bucharest, Romania*

[e] *JINR Dubna, Russia*

[f] *University of Tokyo, Japan*

[g] *Kirchhoff-Institut für Physik, Heidelberg, Germany*

for the ALICE Collaboration

We present measurements of the energy loss of pions and electrons in drift chambers operated with a Xe,CO_2(15%) mixture. The measurements are carried out for particle momenta from 1 to 6 GeV/c using prototype drift chambers for the ALICE TRD. Microscopic calculations are performed using input parameters calculated with GEANT3. These calculations reproduce well the measured average and most probable values for pions, but a higher Fermi plateau is required in order to reproduce our electron data. The widths of the measured distributions are smaller for data compared to the calculations. The electron/pion identification performance using the energy loss is also presented.

Key words: drift chambers, xenon-based gas mixture, ionization energy loss, electron/pion identification, transition radiation detector
PACS: 29.40.Cs, 29.40.Gx

1 Introduction

The ALICE Transition Radiation Detector (TRD) [1] is designed to provide electron identification and particle tracking in the high-multiplicity heavy-ion collisions at the LHC. To achieve the challenging goals of the detector, accurate pulse height measurement in drift chambers operated with Xe,CO_2(15%) over the drift time of about 2 μs is a necessary requirement. For such precision measurements, it is of particular importance first to collect [2] and then to properly amplify [3] all the charge deposited in the detector. For electrons, the transition radiation (TR), produced in an especially designed raditor, is overimposed on the ionization energy loss and helps crucially in improving the electron/pion separation. A factor of 100 pion rejection for 90% electron efficiency is the design goal of the detector and was demonstrated with prototypes [1]. The measurements of ionization energy loss (dE/dx) in TRD will contribute to the identification of other charged particles, supplementing the identification power of the ALICE Time Projection Chamber. A good understanding of dE/dx in the TRD is a prerequisite for high-precision simulations of the detector performance in terms of TR.

Existing measurements of dE/dx in Xe-based mixtures [4–6] are scarce and have good precision on an absolute energy scale only in one case [6]. Calculations of dE/dx can reproduce the measured data, in particular for Xe-based mixtures [6,7]. Ref. [8] is an excellent early overview on energy loss measurements and calculations as well as on its application to particle identification. For a more recent account, see ref. [9].

We report on dE/dx measurements performed during prototype tests for the ALICE TRD. The experimental setup and method of data analysis are described in the next section. We then present the basic ingredients of our simulation code and discuss the general outcome. The measured data in comparison to the calculations are presented in Section 4.

2 Experimental setup

The results are obtained using prototype drift chambers (DC) with a construction similar to that anticipated for the final ALICE TRD [1], but with a smaller active area (25×32 cm^2). To allow the measurement of the pure ionization energy loss for electrons, no radiator was used for the present measurements. The prototypes have a drift region of 30 mm and an amplification region of 7 mm. Anode wires (W-Au) of 20 μm diameter are used, with a pitch of 5 mm. The cathode wires (Cu-Be) have 75 μm diameter and a pitch of 2.5 mm. We read out the signal on a segmented cathode plane with rectangular pads of 8 cm length and 0.75 cm width. The entrance window (25 μm aluminized Kapton) simul-

[1] Corresponding author: GSI, Planckstr. 1, 64291 Darmstadt, Germany; Email: A.Andronic@gsi.de; Phone: +49 615971 2769; Fax: +49 615971 2989.
[2] On leave from NIPNE Bucharest, Romania.

taneously serves as gas barrier and as drift electrode. We operate the drift chambers with the standard gas mixture for the TRD, Xe,CO_2(15%), at atmospheric pressure. The gas is recirculated using a dedicated gas system. Our nominal gain of about 4000 is achieved with an anode voltage of 1.55 kV. For our nominal drift field of 0.7 kV/cm, the detector signal is spread over about 2 μs.

We use a prototype of the charge-sensitive preamplifier/shaper (PASA) especially designed and built for the TRD in 0.35 μm CMOS technology. It has a noise on-detector of about 1000 electrons r.m.s. and the FWHM of the output pulse is about 100 ns for an input step function. The nominal gain of the PASA is 12 mV/fC, but during the present measurements we use a gain of 6 mV/fC for a better match to the range of the employed Flash ADC (FADC) system with 0.6 V voltage swing. The FADC has adjustable baseline, an 8-bit non-linear conversion and 20 MHz sampling frequency. The FADC sampling was rebinned in the off-line analysis to obtain 100 ns time bins as for the final ALICE TRD [1]. The data acquisition (DAQ) was based on a VME event builder and was developed at GSI [15].

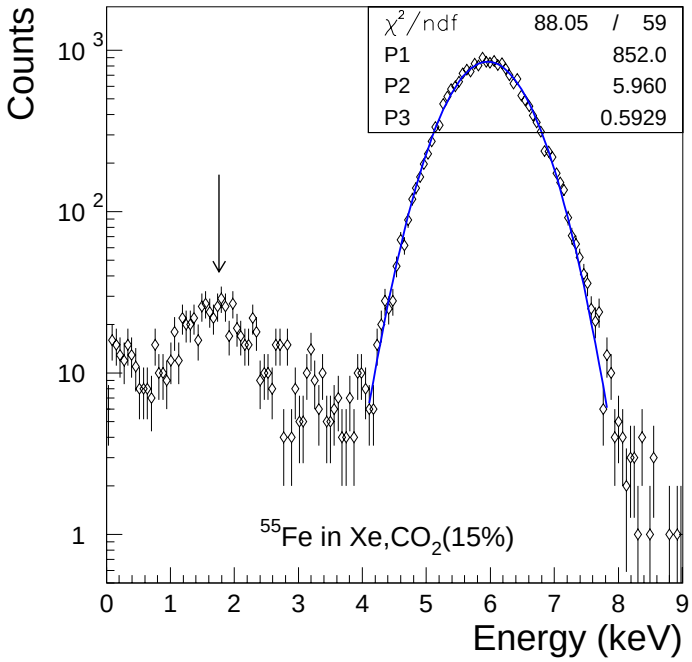

Fig. 1. ^{55}Fe spectrum in Xe,CO_2(15%). A Gaussian fit of the main peak of 5.96 keV is also plotted. The arrow marks the expected position of the escape peak of Xe at 1.76 keV.

The energy calibration of the detectors has been performed using a ^{55}Fe X-ray source. A spectrum of the integrated ^{55}Fe signal is shown in Fig. 1 for our nominal anode voltage of 1.55 kV. The spectrum has been calibrated with one gain parameter (the baseline is obtained using empty presamples, there is no offset) using the main peak of 5.96 keV. The arrow marks the expected position of the escape peak of Xe at 1.76 keV, (the weighted average of the L lines of Xe is 4.202 keV), which is in good agreement with the measure-

ments. The energy resolution for the main peak is 23% FWHM.

Four identical drift chambers were used for the beam measurements, without any radiator in front. The variation of the gas gain for each individual chamber is within 10% and is calibrated away. The measurements are carried out at momenta of 1, 1.5, 2, 3, 4, 5, and 6 GeV/c at the T10 secondary beamline of the CERN PS [16]. The momentum resolution is $\Delta p/p \simeq 1\%$. The beam intensity is up to 3000 particles per spill of about 1 second. As the beam diameter was of the order of 2.5 cm, we usually limited the readout of the DC to 8 pads. This also minimizes data transfer on the VSB bus connecting the FADC and the event builder. The beam is a mixture of electrons and negative pions. Similar sample sizes of pion and electron events are acquired within the same run via dedicated triggers. For the present analysis we have selected clean samples of pions and electrons using coincident thresholds on two Cherenkov detectors and on a lead-glass calorimeter [17]. The incident angle of the beam with respect to the normal to the anode wires (drift direction)is 15° to avoid gas gain saturation due to space charge [3].

3 Procedure and inputs for energy loss calculations

The calculations are performed using a standalone Monte Carlo program especially written for this purpose. In general, the ingredients needed for calculating the ionization energy loss of an incoming charged particle in any material are just the number of the primary inelastic collisions and the spectrum of the energy transfer in these collisions. These quantities depend on the particle type and momentum (or Lorentz factor γ) and on the medium traversed. In our case, the inputs were extracted from GEANT3 [10].

The energy spectrum of primary electrons released in inelastic collisions of a minimum ionizing particle (MIP, γ=4) is presented in Fig. 2. In GEANT3 an implementation of the photoabsorption ionization model [8] is used to calculate this spectrum. This is the integral spectrum of the number of the inelastic collisions per centimeter with an energy transfer greater than E, $(\mathrm{d}N/\mathrm{d}x)_{>E}$. For comparison, we plot also, arbitrarily normalized, the pure Rutherford spectrum, which, in the integral form, has a $1/E$ dependence. The calculated spectrum has structures coresponding to the atomic shells (most conspicous are the N and M shells of Xe) and approaches the Rutherford limit for large values of the energy transfer.

The total number of primary collisions per cm of traversed gas, N, is the value corresponding to the lower limit of the energy transfer and is 19.3 for our case. Note that this number is much smaller compared than the values quoted in earlier works: 48 by Ermilova et al. [11] and 44 by Sauli [12] or Zarubin [13]. On the other hand, Va'vra [9] has recently deduced that N is about 25 for Xe. The lowest value of the energy transfer in the GEANT3 spectrum is 11.26 eV [10]. Since the value of the lowest ionization potential for Xe is I=12.13 eV (for CO_2 I=13.81 eV) [14], we restrict for our simulations the lowest energy transfer to this value of 12.13 eV, while keeping unchanged the number of primary

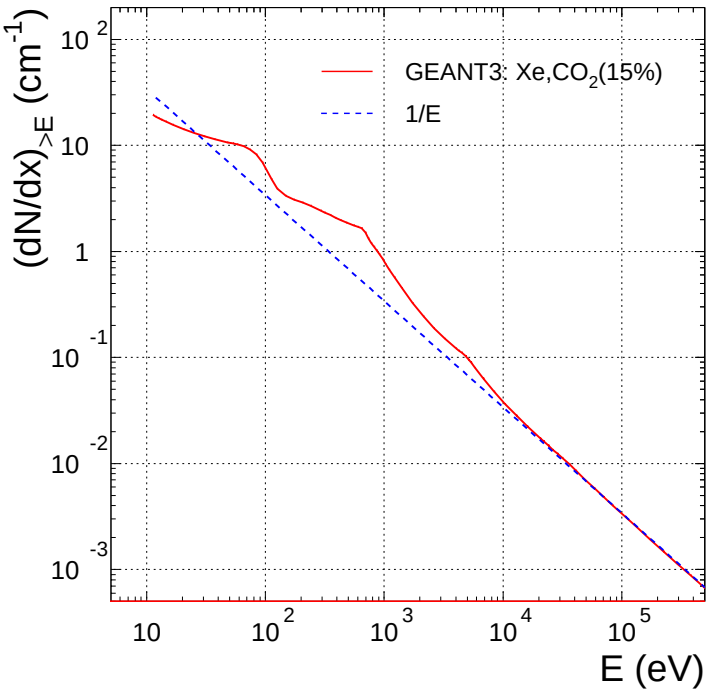

Fig. 2. The integral spectrum of the energy transfer in primary collisions.

collisions. This threshold leads to an increase of the simulated average energy loss by 4% compared to the case when 11.26 eV would be the lowest allowed energy transfer.

In addition to the material-dependent values presented above, one has to specify their dependence on the incoming particle's Lorentz factor, γ. We assume that the spectral shape of the energy transfer is independent of γ and only the total number of primary collisions depends on γ. This factor, f, is the relative increase of N with respect to the value for MIP. Its dependence, as extracted from GEANT3, is presented in Fig. 3 for our gas mixture. Note that in GEANT3 the Fermi plateau corresponds to a number of primary inelastic collisions 1.55 times larger with respect to MIP. This value is sizeably larger than the value of 1.36 calculated by Ermilova et al. [11]. As we shall see below, our measurements favor an even higher Fermi plateau than that extracted from GEANT3, of about 1.61. This is shown by the dashed line in Fig. 3. For a given detector thickness D and for a given γ value, the spectrum presented in Fig. 2 is sampled on average $N_{tot} = NDf(\gamma)$ times. For an individual track, the actual number of inelastic collisions is obtained by sampling a Poissonian distribution with the average N_{tot}.

The δ-rays (energetic electrons produced in inelastic collisions) are tracked for energies above 10 keV. This class is what we denote here generically δ-rays (there is no accepted threshold above which a primary electron is called δ-ray). For these electrons the range is

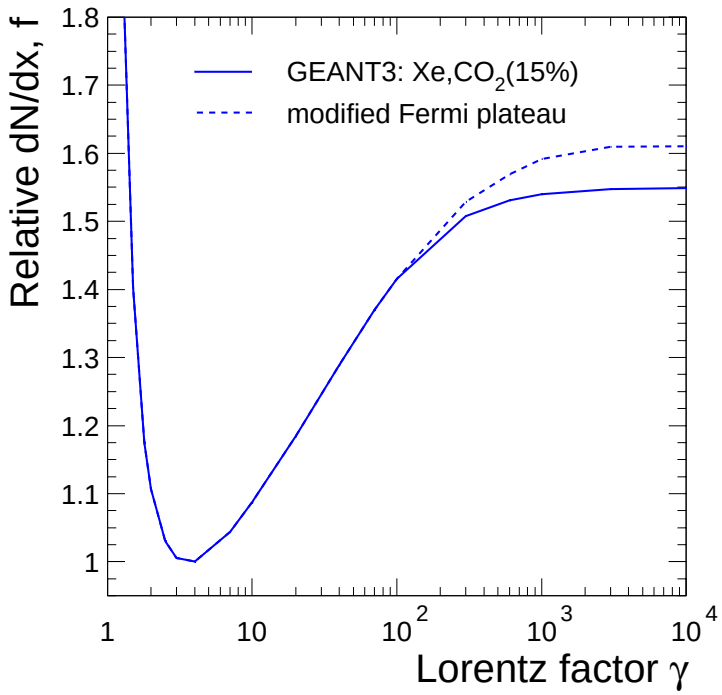

Fig. 3. The dependence of the primary number of inelastic collisions normalized to MIP (γ=4) on the Lorentz factor. The full line is obtained using GEANT3, the dashed line is for an increased value of the Fermi plateau that best reproduces our measurements.

calculated according to the formula [14]:

$$R(E) = AE\left(1 - \frac{B}{1+CE}\right), \tag{1}$$

with A=5.37·10^{-4} gcm^{-2}keV^{-1}, B=0.9815, and C=3.123·10^{-3} keV^{-1} [14]. E is the energy of the δ-ray. For instance, for our gas mixture, the range is 0.52 mm for 10 keV and 27.4 mm for 100 keV δ-rays. We assume that the δ-rays move on a straight trajectory co-linear with the parent particle. If a δ-ray was produced in the detector depth such that the range is greater than the remaining path length of the parent track in the detector, the γ of the δ-ray is calculated and its energy deposit is treated as for an independent track and added to the parent track. For our detector geometry, 15.3% of the tracks of 2 GeV/c pions have a δ-ray above 10 keV. Of those, 16.3% (or 2.5% of all the tracks) escape from the detector volume.

In Fig. 4 we present the comparison of the energy loss integrated over the detector thickness, Δ, for pions of 2 GeV/c. The four cases are for: i) all tracks, ii) tracks not containing any δ-ray, ii) tracks with δ-ray, but which are completely absorbed in the detector, and iv) tracks for which one δ-ray escapes the detector. For this last case the energy loss in this example is calculated taking the total energy of the δ-ray. These spectra illustrate the contribution of δ-rays to the well known Landau shape of energy loss in thin detectors:

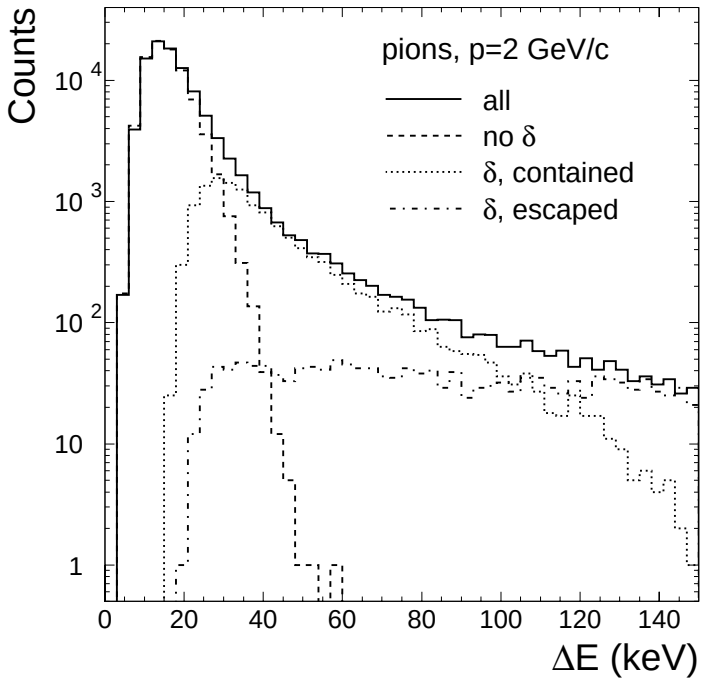

Fig. 4. Calculated integrated energy loss in our detector for 2 GeV/c pions for: i) all tracks (full histogram), ii) tracks which do not have any δ-ray (dashed), iii) tracks with δ-rays which are contained in the detector (dotted) and iv) tracks for which a δ-ray has escaped the detector volume (dot-dashed).

the tail originates from the tracks for which one or more δ-rays have been produced [6]. Depending on the detector thickness, some of those will escape the detection volume. This leads to the distinction between the energy loss and the energy deposit, which comprises only the detected signal (and is obviously smaller than the energy loss). The flat energy loss distribution for tracks containing escaped δ-rays (dot-dashed histogram) is the result of the random distribution of these δ-rays in the detector thickness: the lower energy δ-rays escape only if they are produced at the end of the path of the parent particle in the detector, while the very energetic ones escape no matter where they are produced.

4 Results and discussion

In Fig. 5 we present the measured distributions of energy loss for pions and electrons for the momentum of 2 GeV/c. Our high-statistics measurements with FADCs with large dynamic range make available for the first time complete energy loss spectra. A very good agreement between data and calculations is seen for the case of δ-rays escaping the detector volume. As noted above, those δ-rays influence only the tails of the distributions. This is the reason why the most probable value (MPV) of the spectrum and not its mean value is most commonly used to characterize the energy loss in thin detectors. From here on

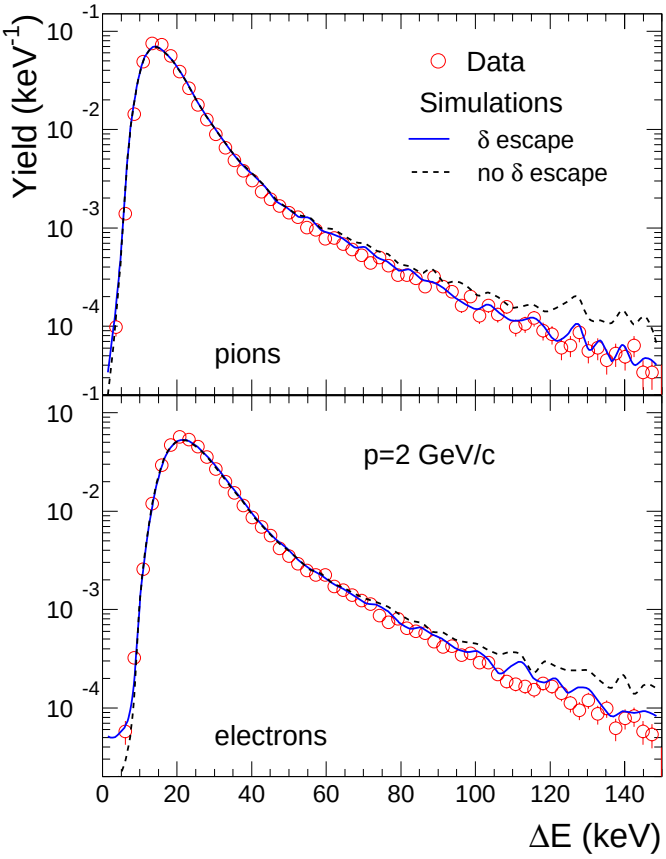

Fig. 5. Spectra of the energy loss of pions and electrons for the momentum of 2 GeV/c. The symbols represent the measurements. The lines are the simulations, with (continuous line) and without (dashed line) taking into account the finite range of δ electrons.

we consider only the simulated results taking into account the tracking of escaped δ-rays. The measurements for all momenta are presented in Fig. 6 together with simulations. One can notice that, due to the relativistic rise of the pions, the separation between the pions and electrons is reduced as a function of momentum. This is the reason why one employs the extra contribution of transition radiation in order to achieve a good electron/pion identification with a TRD. In general, the agreement between data and calculations is good for all momenta, but on a linear scale one can already notice that the widths of the distributions are larger in case of simulations (see below). The calculated distributions are for the modified Fermi plateau. All the measured spectra are available at the web page of our collaboration [18]. Note that, due to the track incidence at 15° with respect to the normal incidence, the distributions correspond to an effective detector thickness of 3.83 cm.

In Fig. 7 we present the momentum dependence of the energy loss values for electrons and pions, for two cases: MPVs and average values. The MPVs are extracted from fits with a convolution of a Landau function and a Gaussian. The measured data are compared to the results of simulations. The errors on the data represent an estimated 2% point-

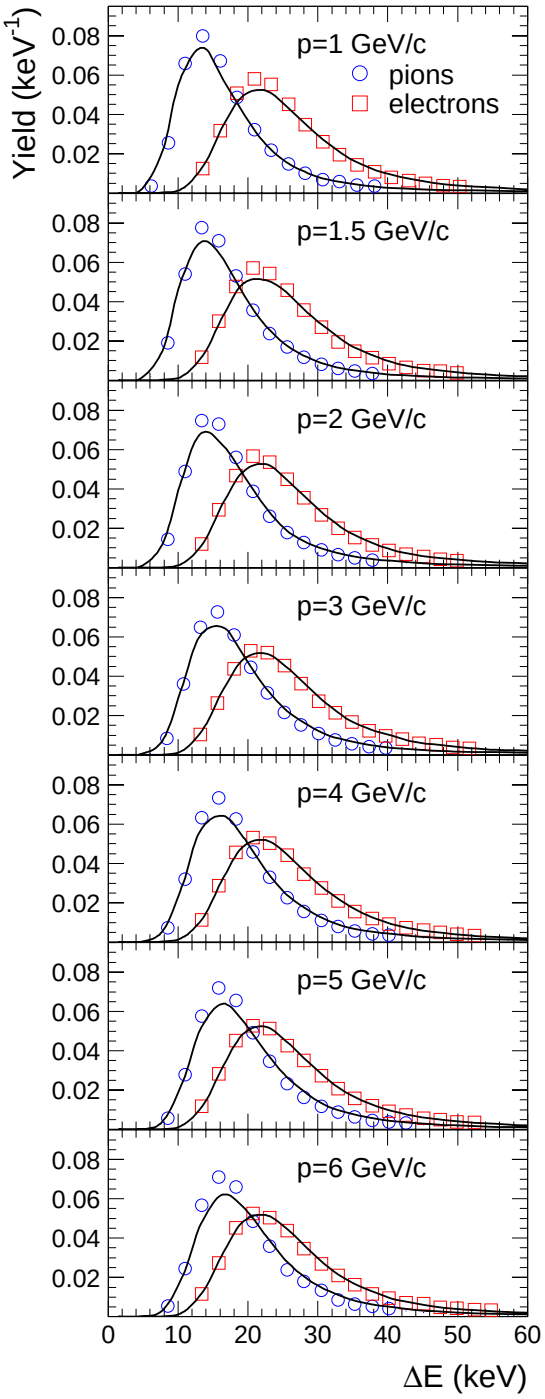

Fig. 6. The energy loss distributions of pions and electrons for momenta of 1 to 6 GeV/c. The symbols represent the measurements, the lines are the simulations.

to-point accuracy, originating from minute changes of the gas composition and pressure. We estimate an overall uncertainty of the absolute energy calibration of about 5%. The statistical error of the Landau fit is negligible. As noted earlier, for our momentum values,

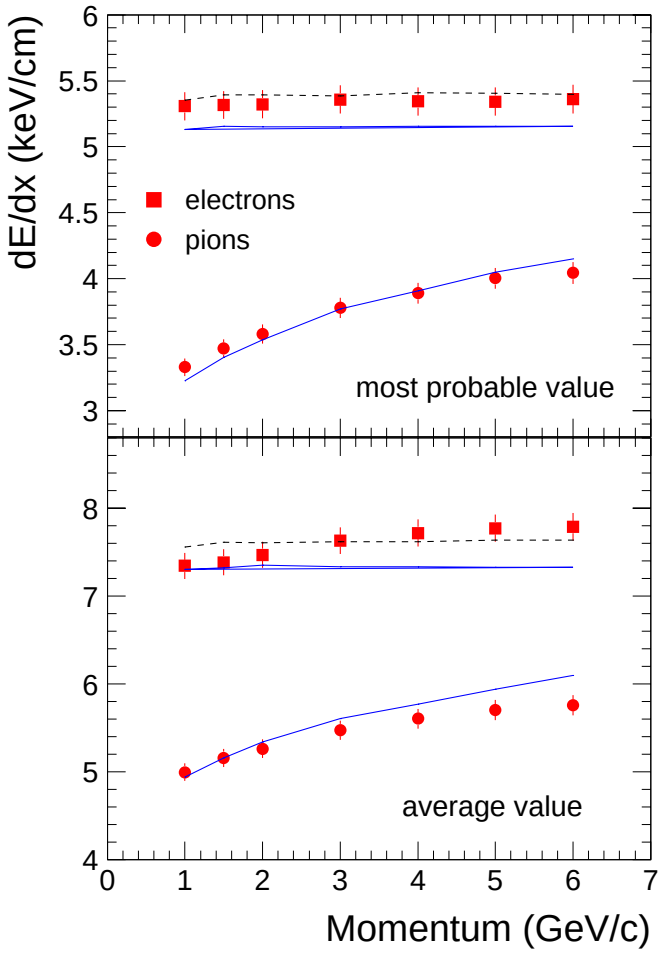

Fig. 7. Momentum dependence of the most probable and the average value of the energy loss for pions and electrons. The symbols are measurements, the lines are calculations (dashed line for the modified Fermi plateau).

the pions are in the regime of the relativistic rise, while the electrons are at the Fermi plateau. These two regimes are reflected in the measured values of the energy loss. Note that our average values for electrons are lower than those reported by Fischer et al. [4], who measured a value of about 9 keV/cm at the Fermi plateau. Appuhn et al. [19] have reported for electrons even larger values of about 12 keV/cm, with a slightly increasing trend for the same momentum range as ours.

The calculations reproduce well the absolute magnitude and the general trends of the data, however, in case of electrons, only with the modified value of the Fermi plateau. The calculations show a more pronounced relativistic rise than the measurements. Also, in case of the average values, the calculations indicate that the Fermi plateau is reached for the electrons for all momentum values, while the data show a slight increase for momenta below 2 GeV/c. Despite the above-mentioned 5% overall uncertainty of the measured values, it is evident that the calculations cannot consistently explain the measured values

for pions and electrons unless one introduces the modified Fermi plateau.

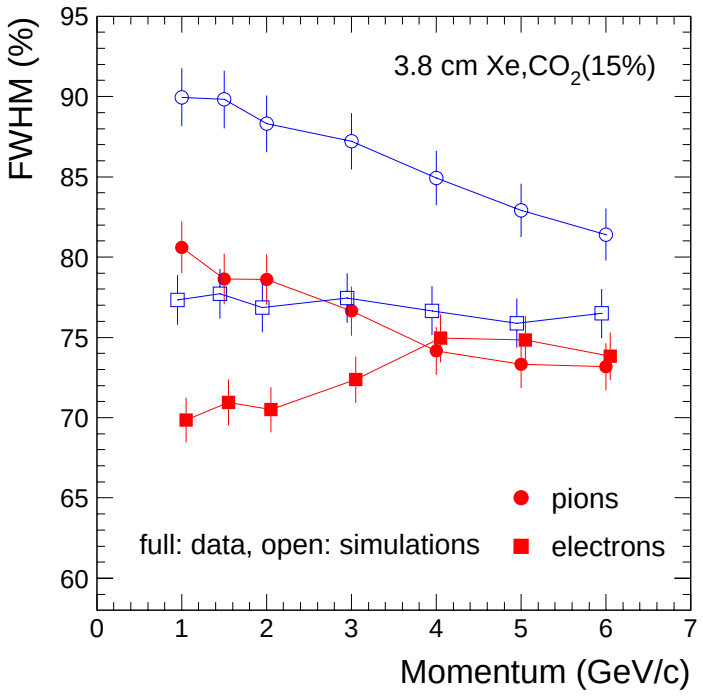

Fig. 8. Momentum dependence of the FWHM value of the energy loss normalized to MPV for pions and electrons. Full symbols are measurements, open symbols are calculations.

The comparion of the measured and simulated values of the FWHM of the energy loss spectra, normalized to MPV, is shown in Fig. 8 for pions and electrons as a function of particle momentum. The FWHM is determined by the magnitude of the ionization, in particular by the average number of primary inelastic collisions. For pions, as a consequence of the relativistic rise, one expects that the FWHM is decreasing as a function of momentum and this is indeed the trend of our measured values. For electrons, due to their constant energy loss, the FWHM is expected to be constant, but the measurements show a slight increase as a function of momentum. This is not quantitatively understood, but Bremsstrahlung is the only candidate to explain such a behavior. Our measured values for pions are larger than those reported in ref. [20] by about 15%.

The calculations reproduce the measured trend for pions, but show clearly larger values of FWHM. The expected constant value of FWHM for electrons is confirmed by the calculations. Bremsstrahlung is not included for the simulated events. Larger FWHMs in case of calculations may be a consequence of too low a number of primary inelastic collisions predicted by GEANT. Obviously, one can not increase this number unconditionally. The spectrum of the energy transfer has to be changed in this case too, otherwise the average values of dE/dx would no longer be in agreement with the measurements. As emphasized by the authors of GEANT3 [10], the shape of the energy transfer spectrum at low energy is strongly dependent on the choice and treatment of the photo-absorption cross sections. If the FWHM is only determined by the number of primary collisions, a simple Poisson

scaling implies that about 25 primary collisions per cm would be required for an agreement between our measurements and the simulations in case of pions. This value is identical to the one inferred by Va'vra [9]. Another possibility is that for the measurements the Penning effect increases the secondary electron statistics [13,21]. We note that similarly larger widths of simulated distributions compared to measurements are also apparent in ref. [7].

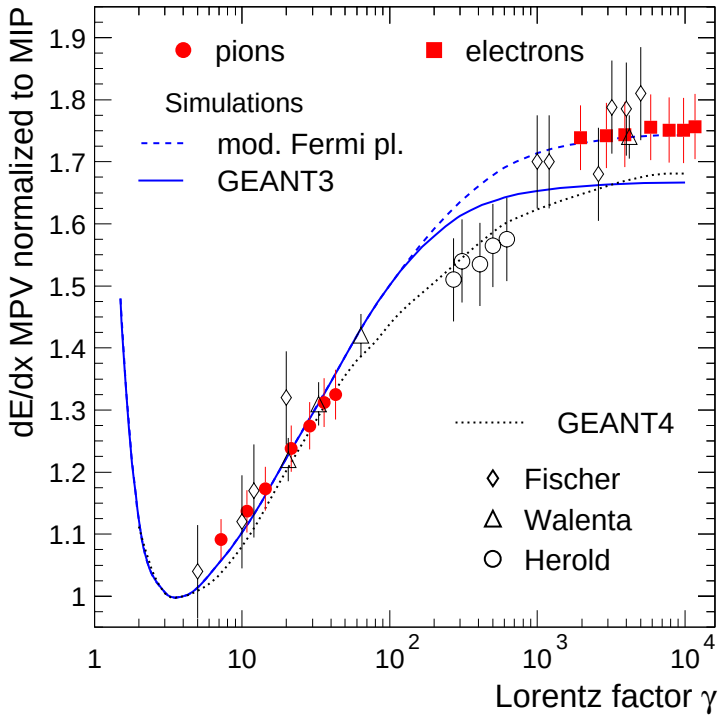

Fig. 9. Relativistic rise of the most probable value of the energy loss. Our values (full symbols) are compared to calculations and to the measurements of Fischer et al. [4], Walenta et al. [5] and Herold et al. [6]. The dashed line is the result of GEANT4 calculations [7].

In Fig. 9 we present the relativistic rise of the most probable value of the energy loss. Our data are compared to other measurements [4–6] and to calculations. For this relative comparison, we have normalized our measured value for 3 GeV/c pions (γ=21) to the calculations. Note that the absolute MPVs of data and calculations agree perfectly at this momentum value (see Fig. 7). The agreement with existing measurements is very good. In particular, we would like to emphasize the perfect agreement with the Fermi plateau value of Walenta et al. [5]. As expected from the previous comparisons, the calculations reproduce the data well, but only in case of the modified Fermi plateau. The results of GEANT4 calculations [7] are included as well. The value of the Fermi plateau in GEANT4 is very close to the GEANT3 case and, as a consequence, underpredicts our measurements. The approach to the plateau is more gradual in case of GEANT4 and this agrees with the measurements of Herold et al. [6], which are clearly overpredicted by our calculations. A Fermi plateau of about 1.98 was calculated [4] using the density effect correction of Sternheimer and Peierls [22]. On the other hand, Cobb et al. [23] have calculated a value

of 1.73, very close to our measured value. Note that the value of the Fermi plateau in the case of MPV, 1.75, is larger compared to the corresponding value for the average energy loss, 1.61 (which is obviously identical to the input value for the Fermi plateau of the number of primary collisions), and the onset of the plateau starts at somewhat larger values of γ (see also Fig. 3) [24].

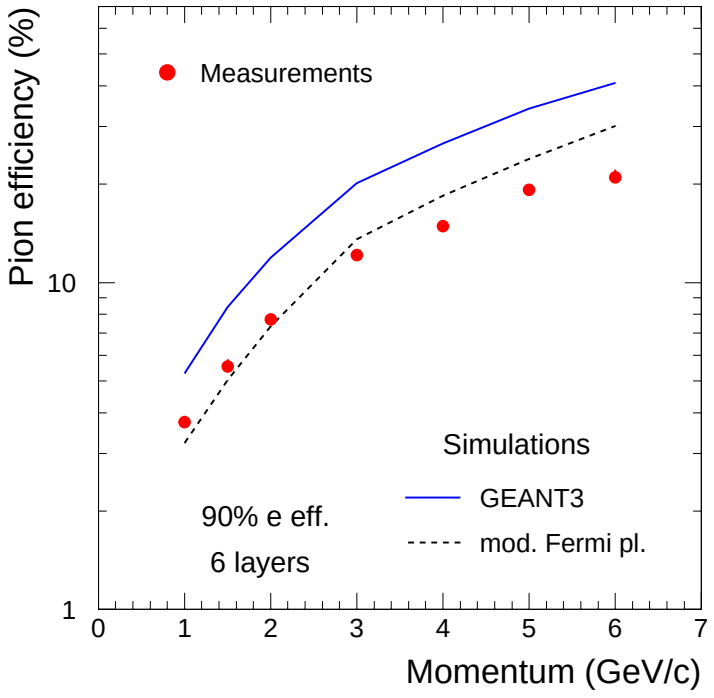

Fig. 10. The momentum dependence of the pion efficiency for 90% electron efficiency. The measurements for 4 layers are used to calculate the expected performance for 6 layers. The lines are the results of simulations.

The results presented above allow the calculation of the electron/pion rejection using pure dE/dx measurements. The results are presented in Fig. 10. A likelihood method [25] on the total energy loss spectra (see Fig. 7) has been used to extract the pion efficiencies for 90% electron efficiency. The measured experimental data for 4 layers has been used to calculate the expected performance for the final ALICE TRD configuration with 6 layers. The experimental errors are of the order of the dimension of the points. The data are compared to the performance extracted from the simulations using an identical procedure. Clearly, the modified Fermi plateau is needed in order to explain the measured pion efficiencies. Moreover, as a result of the faster relativistic rise in the simulations compared to the data, the simulations show a degradation of the pion rejection performance which is steeper than the measurements. The larger widths of the simulated Landau distributions play a role, too.

In ALICE TRD the contribution of TR is significantly improving the electron identification performance [17]. Pion efficiencies below 1% have been achieved in tests with prototypes [17]. However, particle identification using dE/dx will be used for other charged

particles, for which truncated means could be a more advantageous way to exploit the measured signal. In case of electron/pion separation, the comparison of measurements and calculations in terms of pure dE/dx is just a necessary step in understanding the contribution of TR, in particular the comparison between measurements and simulations of the TRD performance.

5 Summary

We have reported measurements of ionization energy loss in drift chambers operated with Xe,CO_2(15%), carried out using prototype drift chambers for the ALICE TRD. Pions and electrons with momenta from 1 to 6 GeV/c were studied. Our high-statistics measurements with FADCs with large dynamic range make available for the first time complete energy loss spectra. Our measured relativistic rise agrees well with existing measurements. The measured distributions are in general well reproduced using microscopic calculations with GEANT3 input parameters, but a modified value of the Fermi plateau (an increase from 1.55 to 1.61) is needed to explain the electron data. The calculations show wider distributions compared to the measurements, suggesting that the number of primary collisions is too low in the standard GEANT3 input values. Apparently, all the noticed discrepancies between data and GEANT3 will apply in case of GEANT4, too.

Acknowledgments

We acknowledge A. Radu and J. Hehner for the skills and dedication in building our detectors. We acknowledge useful discussions with S. Biagi. We would also like to acknowledge P. Szymanski for help in organizing the experiment and A. Przybyla, and M. Wensveen for technical assistance during the measurements. We thank N. Kurz for assistance with the data acquisition.

References

[1] ALICE TRD Technical Design Report, CERN/LHCC 2001-021, October 2001; *http://www-alice.gsi.de/trd/tdr*.

[2] A. Andronic et al., Nucl. Instr. Meth. Phys. Res. A **498** (2003) 143.

[3] A. Andronic et al., accepted for publication in Nucl. Instr. Meth. Phys. Res. A (2003) .

[4] J. Fischer, S. Iwata, V. Radeka, C.L. Wang, W.J. Willis, Nucl. Instr. Meth. **127** (1975) 525.

[5] A.H. Walenta, J. Fischer, H. Okuno, C.L. Wang, Nucl. Instr. Meth. **161** (1979) 45.

[6] W.D. Herold, J. Egger, H. Kaspar, F. Pocar, Nucl. Instr. Meth. **217** (1983) 277.

[7] J. Apostolakis, S. Giani, L. Urban, M. Maire, A.V. Bagulya, V.M. Grichine, Nucl. Instr. Meth. Phys. Res. A **453** (2000) 597.

[8] W.W.M. Allison and J.H. Cobb, Ann. Rev. Nucl. Part. Sc. **30** (1980) 253.

[9] J. Va'vra, Nucl. Instr. Meth. Phys. Res. A **453** (2000) 262.

[10] GEANT 3.21 Package, CERN Program Library W5013 (section PHYS334).

[11] V.C. Ermilova et al., Nucl. Instr. Meth. **145** (1977) 555.

[12] F. Sauli, CERN Report 77-09 (1977).

[13] A.V. Zarubin, Nucl. Instr. Meth. Phys. Res. A **283** (1989) 409.

[14] W. Blum and L. Rolandi, Particle Detection with Drift Chambers, Springer-Verlag, 1994.

[15] H.G. Essel and N. Kurz, IEEE Trans. Nucl. Sci. vol. **47** (2000) 337.

[16] CERN PS, *http://psdoc.web.cern.ch/PSdoc/acc/pscomplex.html*.

[17] A. Andronic et al., IEEE Trans. Nucl. Sci. vol. **48** (2001) 1259 [nucl-ex/0102017].

[18] ALICE TRD Homepage: *http://www-alice.gsi.de/trd*.

[19] R.D. Appuhn, K. Heinloth, E. Lange, R. Oedingen, A. Schlösser, Nucl. Instr. Meth. Phys. Res. A **263** (1988) 309.

[20] A.P. Onuchin and V.I. Telnov, Nucl. Instr. Meth. **120** (1974) 365.

[21] S. Biagi, private communication.

[22] R.M. Sternheimer and R.F. Peierls, Phys. Rev. **B 3** (1971) 3681.

[23] J.H. Cobb, W.W.M. Allison, J.N. Bunch, Nucl. Instr. Meth. **133** (1976) 315.

[24] F. Lapique and F. Piuz, Nucl. Instr. Meth. **175** (1980) 297.

[25] A. Büngener, B. Koppitz, R. van Staa, P. Stähelin, M. Holder, Nucl. Instr. Meth. **214** (1983) 261.